Property enhancement of cold sprayed Al-diamond MMC coating by using core-shelled diamond reinforcements

Shuo Yin, Rocco Lupoi
Trinity College Dublin, The University of Dublin, Department of Mechanical and Manufacturing Engineering, Parsons Building, Dublin 2, Ireland
yins@tcd.ie, lupoir@tcd.ie

Chaoyue Chen
State Key Laboratory of Advanced Special Steels, School of Materials Science and Engineering, Shanghai University, Shanghai, 200072, China
cchen1@shu.edu.cn

Abstract (Required)

Super wear-resistance and light-weight Al-based metal matrix composite (MMC) coatings were produced using cold spray. Cu-Ni coated diamond with core-shell structure and pure diamond were used as reinforcing particles, respectively. The experimental results indicate that the metallic Cu-Ni shell as a 'buffer layer' effectively prevented the fracture of the diamond core upon impact, while the pure diamond suffered from severe fracture during cold spray deposition. The Cu-Ni coated diamond particles were found to be much easier to deposit than pure diamond particle due to formation of metallurgical bonding between the Cu shell and Al matrix which facilitates the deposition of Cu-Ni coated diamond particles. The tribological study indicates that both diamond reinforced MMC coatings exhibited super wear resistance performance. The coating reinforced with Cu-Ni coated diamond had better wear resistance performance than the one reinforced with pure diamond due to the higher diamond content and involvement of Cu and Ni.

Introduction

Cold spray is an emerging coating and additive manufacturing technology [1]. In this process, micro-scale powders are accelerated by a supersonic gas passing through a de-Laval nozzle and subsequently impact onto a substrate to form a coating or bulk deposit [2]. Metals [3], metal matrix composites (MMCs) [4] and certain ceramics [5] have been successfully deposited onto various substrates via cold spray without exceeding their melting points. Defects encountered in the high-temperature deposition processes such as oxidation, thermal residual stress and phase transformation, can be effectively avoided [6–10]. Cold spray can fabricate materials with complex structures, produce thin-film coatings, and repair damaged components [11,12]. Al and its alloys have been widely used in the sectors of aerospace, automotive and construction due to their low density and excellent corrosion-resistance property. However, as soft metals, Al and Al alloys have less favorable wear-resistance performance and hence always suffer from serious erosion during routine service. Al-based MMCs reinforced by hard particles could then be an option to solve this problem. With additional hard particles, Al-based MMCs have improved wear-resistance properties as compared to pure Al and Al alloys. Cold spray has shown great potentials in producing Al-based MMC coatings.

To date, a number of works have been done to study the wear resistance properties of cold sprayed Al-based MMC coatings. Previous studies have shown that cold sprayed Al-based MMC coatings can reduce the wear rate by an order of magnitude as compared with pure Al and Al alloy coatings [13–15]. However, the state of the art suggests that, the commonly used reinforcing particles for Al-based MMC coatings (i.e. Al_2O_3 [16–18], SiC [14,15,18], TiN [19,20], BN [21,22] and B4C [23]) are not hard enough, which limits the further improvement of coating wear-resistance. On the other hand, studies also suggest that the powder feedstock used for MMC coating deposition (i.e., mechanical mixed powders and ball milled powders) are not sophisticated. The mechanically pre-mixed powders frequently lead to a reduction of the reinforcement content in the deposits as compared to in the original feedstock [15,22]. Ball-milling procedure always results in degrading of feedstock particles, which is harmful to the coating cohesion strength [24,25]. Therefore, it is highly important to find a better powder mixture for cold spray MMC coating deposition

Considering the current challenges for producing super wear-resistance cold sprayed Al-based MMC coatings, in this paper, we used diamond which is the hardest material in nature as the reinforcing phase for the cold sprayed Al MMC coating fabrication. In addition, in order to facilitate the diamond deposition, sophisticated Cu-Ni coated diamond powders with core-shelled structure was used and mechanically mixed with Al powders to form the feedstock. For comparison, mechanically mixed pure diamond powders and Al powders were also considered in this work. The two types of feedstock were cold sprayed to form diamond-reinforced MMC (DMMC) coatings using nitrogen as the propulsive gas. Following the deposition, the coating microstructure, diamond fraction, deposition efficiency, interfacial bonding features, and wear-resistance properties of the two DMMC coatings were studied and compared with each other.

Experimental methodology

Composite fabrication

Spherical Al (-58+15 μm, Valimet, USA), Cu-Ni-coated diamond (-53+45 μm, Element-Six, Ireland), and pure diamond (-53+45 μm, Element-Six, Ireland) powders were used for cold spray in this work. Fig. 1 shows the morphology of the powders used in this work as observed by secondary electron microscopy (SEM, Carl Zeiss ULTRA, Germany). For better understanding the inner structure of the Cu-Ni-coated diamond particle, the cross-sectional SEM image prepared by focused ion beam (FIB, DB235, FEI Strata, USA) is shown as insert in Fig. 1b [4,26]. The Cu-Ni-coated diamond particle consists of a diamond core, an electroless Ni nanolayer and an electroless thin Cu layer with only few microns. From the cross-sectional view, the electroless Ni nanolayer on the diamond surface and the outside Cu layer can be clearly seen. According to the supplier's information, the weight ratio of the diamond to both metals in a single particle is approximately 1:1.

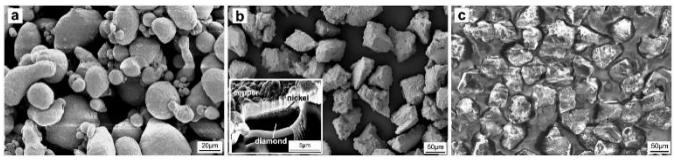

Figure 1: Feedstock powders used in this work. (a) morphology of Al powders, (b) morphology of Cu-Ni-coated diamond powders and a cross-sectional view prepared by FIB as insert, and (c) morphology of pure diamond powders.

The two types of diamond powders were mechanically mixed with the Al powders at the weight ratio 1:1, respectively. The estimated volume fractions of diamond are 25% in the feedstock with Cu-Ni coated diamond mixture and 39% in the feedstock with pure diamond mixture. The mixed powders were deposited onto 25 mm × 25 mm Al substrates using an in-house cold spray system (Trinity College Dublin, Ireland). Nitrogen at the pressure of 3.0 MPa and temperature 400 °C was used as the propulsive gas. The standoff distance and nozzle traverse speed were defined as 35 mm and 50 mm/s, respectively. For the convenience of the following result demonstration and discussion, the cold sprayed DMMC coatings were named as DMMC-1 for the Cu-Ni coated diamond reinforced coating and DMMC-2 for the pure diamond reinforced coating, respectively. In order to understand the deposition feature of a single diamond particle, the single particle deposition test was also conducted. The two types of diamond powders were deposited onto polished Al substrates (made by cold spray) at a high traversal speed of 200 mm/s.

Materials characterization

The bonding ratios of the diamond particles on the Al substrates were measured based on the single particle deposition test. The bonding ratio was calculated using the following expression:

$$\mathrm{BR} = \frac{\mathrm{N_D}}{\mathrm{N_T}}$$

where BR is the bonding ratio, ND is the number of deposited particles and NT is the total impacting particles (sum of the number of deposited particles and craters). In order to assess the coating microstructure, all samples were prepared using standard metallographic procedures. The cross-section of the polished samples was studied using SEM. The diamond volume content in the coatings were calculated based on binary image analysis. The binary image analysis was performed on the cross-sectional micrographs using the imaging analysis software, image J. For each sample, five photographs were taken from the polished cross-section and the calculated data were averaged. In order to study the bonding mechanism between the Cu-Ni-coated diamond particles and Al matrix, transmission electron microscopy (TEM, Titan, FEI, USA) was performed on the Al-Cu interfaces. FIB was used to precisely capture the Cu-Al interface and to prepare the thin foil (<100nm) for TEM analysis. High-resolution TEM (HRTEM) images were analyzed, and fast Fourier transformation (FFT) patterns were taken using Gatan Digital Micrograph to illustrate crystallographic characteristics.

Tribological tests

The wear-resistance properties of the DMMC coatings were tested using POD-2 pin-on-disc tribometer (CSEM Instruments, Switzerland) at room temperature. For accurate measurement of the wear rates, the sample surfaces were polished using diamond solution to 6 μm roughness prior to the test and the samples were then mounted on a carrier disc. A WC-Co ball with a diameter of 5 mm was used as a counterpart under a constant load of 5 N. The disk rotated at a linear speed of 50 mm/s for 1000m with a wear track diameter of 3 mm. In order to determine the coating wear rates, the material volume loss was calculated according to ASTM G 99 standard [27]. The wear rate was then calculated as the volume loss per unit load and per traverse distance. In order to study the wear mechanism, the wear tracks were analyzed by SEM and energy-dispersive X-ray spectroscopy (EDX, Oxford Instruments INCA system, UK).

Results and Discussion

Coating microstructure and single particle deposition

Figure 2 illustrates the general microstructures of the DMMC-1 and DMMC-2 coatings. From Fig. 2a and 2d which show the cross-sections of both coatings, it is seen that diamond reinforcements uniformly dispersed within both coatings. The homogenous distribution of reinforcing particles is known to be beneficial to the MMC coatings properties [28–30]. Apart from this, significant differences also can be noticed when comparing the two coatings. In the DMMC-1 coating, Cu-Ni metal shells can be clearly seen surrounding the diamond cores as represented by the light color. In addition, most of the diamond particles in the DMMC-1 coating had a diameter of approximately 40-50 μm, which is comparable to the diamond core diameter in the original feedstock (-47+40 μm). This fact indicates that most diamond particles did not undergo substantial fracturing during deposition. The reason for this could be the Cu-Ni metal shell which acts as a 'buffer layer' alleviating the impact to the diamond core during deposition

and hence preventing the diamond core from fracture. However, in the DMMC-2 coating, nearly half of the diamond particles had a diameter of approximately 10 - 30 μm, suggesting the occurrence of diamond fracture during the deposition. Another difference is the diamond contents in the coatings. The diamond volume contents in the DMMC-1 coating was 19.17±1.75% with a retainability of 76.68±7 %, while the DMMC-2 coating had a diamond volume fraction of 12.78±1.19 % with a retainability of 32.77±3.05 %. Retainability is defined as the ration of the diamond content in the coating to that in the original feedstock. The comparison of the retainability clearly implies that the Cu-Ni coated diamond was much easier to deposit than the pure diamond and resulted in less much waste of diamond powders.

Fig. 2b and 2e show the surface morphologies of the Al substrates after single particle deposition test with the Cu-Ni coated diamond particles and pure diamond particles. It is seen that all the Cu-Ni coated diamond particles remained intact with only few particles experiencing shell delamination as marked by white arrows. In contrast, most of the pure diamond particles were fractured after deposition. This fact further suggests that the Ni-Cu metal shell can prevent the fracture of diamond core. In addition, the bonding ratio measurements show that the Cu-Ni coated diamond particles had a higher bonding ratio than the pure diamond particles (27.51±3.59% against 20.64±2.40%), which further indicates that the Cu-Ni-coated diamond particles were easier to deposit than the pure diamond particles. Note that fracture diamond particles in the DMMC-2 coating were also considered as deposited particles. Fig. 2c and 2f show the morphology of a single Cu-Ni coated diamond particle and a single pure diamond particle after single particle deposition test. Clearly, the Cu-Ni coated diamond particle well deposited on the Al substrate without any fracture. However, for the pure diamond particle, fracture was clearly seen as marked by white arrow. A large number of diamond fragments can also be observed at the particle surrounding area, indicating the server fracture of the pure diamond particle during deposition. From Fig. 2 b, c, e and f, it is evident that the conclusions drawn from single particle test are in good agreement with those from full coating deposition (Fig. 2a and d).

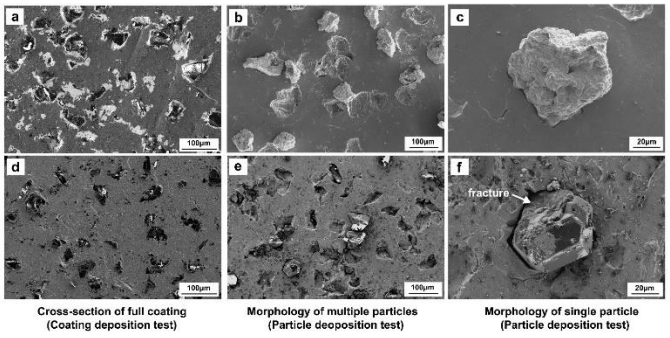

Figure 2: General microstructures of the DMMC-1 and DMMC-2 coatings. (a) cross-sectional view of the DMMC-1 coating, (b) surface morphology of the substrate after single Cu-Ni coated diamond particle deposition test, (c) morphology of a single Cu-Ni coated diamond particle after single particle deposition test, (d) cross-sectional view of the DMMC-2 coating, (e) surface morphology of the substrate after single pure diamond particle deposition test, (f) morphology of a single pure diamond particle after single particle deposition test

Metallurgical bonding between Cu-Ni shell and Al matrix

In conventional cold sprayed MMC coatings, non-metallic reinforcing particles only mechanically embed into soft metal matrix without chemical reaction between each other. Therefore, the deposition efficiency and retainability of non-metallic particles are generally low [31]. However, in this work, as shown in Fig. 2a, b and c, the metallic Cu-Ni shell of the Cu-Ni-coated diamond particle can intimately contact with the Al matrix to form metal-to-metal contact. In this case, it is possible to infer that metallurgical bonding may occur between the Cu-Ni coated diamond and Al matrix through the Cu-Al interface. In order to clarify this hypothesis, a Cu-Al interfacial area cut from the DMMC-1 MMC coating by FIB was studied. Fig. 3a shows the HRTEM images and the corresponding FFT pattern at the Cu-Al interface. Based on the FFT pattern, the lattice spacing was measured to be 0.42 nm, which is comparable to the CuAl2 intermetallic phase. This intermetallic phase clearly indicates the occurrence metallurgical bonding between the Cu shell and Al matrix [32,33]. Further evidence of the occurrence of metallurgical bonding is provided in Fig. 3b showing the STEM image at the Cu-Al interface. As can be seen, the Cu-Al interface was characterized by three different regions. By the aid of localised EDX analysis, it is confirmed that the Al matrix and Cu shell was bridged by a layer of intermetallic phase with a thickness of 70 nm. The atomic ratio between Cu and Al was approximately 1:1 in the intermetallic region, indicating the CuAl2 intermetallic phase, which is consistent with the FFT pattern. The TEM characterization shown in Fig. 3 clearly suggests that the bonding mechanism between the Cu shell and Al matrix was metallurgical bonding. It has been widely known that inter-particle metallurgical bonding can provide high bonding strength. This fact explains why the Cu-Ni coated diamond was much easier to deposit than the pure diamond, and also explains why the retainability and bonding ratio of the Cu-Ni coated diamond were higher. The results presented here also demonstrate that using core-shelled powders as the feedstock for cold sprayed MMC coatings can promote the bonding between the metal matrix and non-metallic particles through the shell-matrix metallurgical bonding and therefore improve the performance of the MMC coatings.

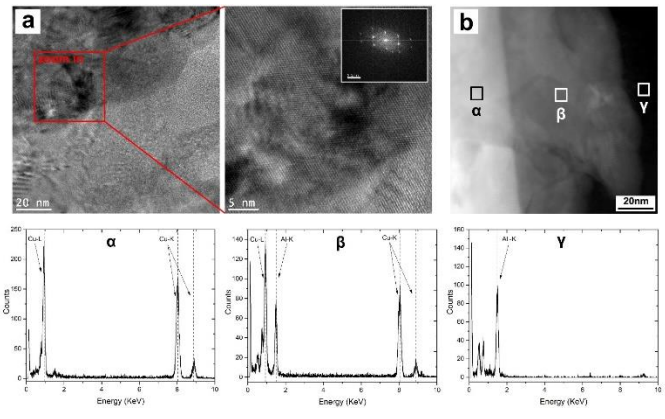

Figure 3: TEM characterization of the Cu-Al interfacial region cut from the DMMC-1 coating. (a) HRTEM image and the corresponding FFT pattern, and (b) STEM image and the corresponding EDX element analysis.

Wear resistance

The wear-resistance properties of the DMMC coatings were also studied int this work, and the results are provided in Fig. 4. Fig. 4a compares the wear rate of the DMMC-1 and DMMC-2 coatings. It is clear that, in both cases, the wear rates of the DMMC-1 coating were lower than those of the DMMC-2 coating, indicating a better wear resistance. The reason for this may be the higher diamond content and better cohesion strength in the DMMC-1 coating than in the DMMC-2 coating. As compared with other cold sprayed Al-based coatings including Al (7×E-3 mm/N·m) [34], Al 2319 (3.6×E-3 mm/N·m) [20], Al 2019+TiN (2.4×E-4 mm/N·m) [20], and Al+Al2O3 (4.8×E-4 mm/N·m) [34], the DMMC coatings produced in this work exhibited significant reduction in wear rate. The comparison clearly indicates the superiority of the DMMC coatings and their super wear resistance performance, particularly the DMMC-1 coating produced with Cu-Ni coated diamond particles.

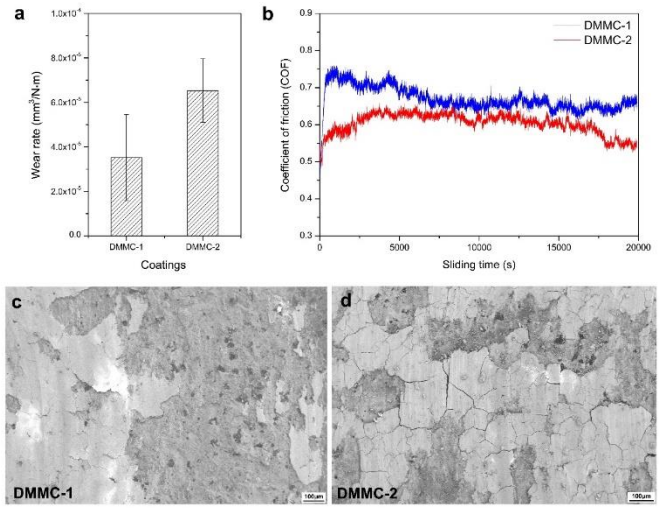

Figure 4: Wear-resistance properties of the DMMC coatings. (a) wear rate, (b) COF, (c) worn surface of the DMMC-1 coating, and (d) worn surface of the DMMC-2 coating

In order to clarify the wear mechanism of the DMMC coatings, the coefficient of friction (COF) and coating worn surfaces are shown in Fig. 4b, c and d. It is seen from Fig. 4b that the COF of the DMMC-1 coating (0.67±0.03) was higher than that of the DMMC-2 coating (0.60±0.03). This may be due to the higher diamond content in the DMMC-1 coating which increase the surface roughness and hence COF. From Fig. 4c and d, it is clearly seen some thick tribofilms on the wear track of both coatings, suggesting the adhesive tribofilm wear mechanism. For the DMMC-1 coating, the EDX mapping shows that the tribofilm was composed of a large amount of W, C, Co and a small amount of Al, Cu and Ni. This fact indicates that the WC-Co pin ball was severely worn during the sliding test due to the super hard diamond reinforcements. The debris worn off from the WC-Co pin ball was crushed during the continuous sliding process and mixed with Al, Cu and Ni coating debris, forming the thick tribofilm. The hard tribofilm can act as a protecting layer preventing the pin ball from further wearing the underneath coating, promoting the wear-resistance performance of the coating. Simultaneously, the tribofilm can also act as a lubricating layer to reduce the COF, explaining why the COF gradually reduced with the sliding distance as shown in Fig. 4b. In addition, cracks and delamination of tribofirm were observed, which indicates the weak cohesion of the tribofirm. For the DMMC-2 coating, thick tribofilm with cracks and delamination was also observed on the wear track. Due to the formation of tribofilm, the COF of the DMMC-2 coating also showed a decreasing trend as the sliding distance increased. The EDX mapping shows that the tribofilm consisted of mainly W, C, Co and a small amount of Al, suggesting that the WC-Co pin ball was also severely worn. As compared with the DMMC-1 coating, the absence of Cu and Ni in the tribofilm may be adverse to the wear resistance performance because Cu and Ni as harder metals than Al can also contributes to the improvement of wear resistance. Therefore, expect for the higher diamond content, the involvement of Cu and Ni in the tribofilm may be another reason for the lower wear rate of DMMC-2 coating.

Conclusions

In this paper, super wear resistance Al-based MMC coatings were produced using cold spray. Two different kinds of diamond powders were used, namely Cu-Ni coated diamond with core-shell structure and pure diamond. The diamond powders were mechanically mixed with Al powders and then deposited on Al substrates. Based on the experimental results, it is found that the metallic shell as a 'buffer layer' effectively prevented the fracture of the diamond core upon impact, while the pure diamond suffered from severe fracture during cold spray deposition. In addition, the core-shelled diamond particles were found to be much easier to deposit than pure diamond particle. Therefore, the diamond retainability in the DMMC-1 coating was much higher than in the DMMC-2 coating. The reason for the this is the formation of metallurgical bonding between the Cu shell and Al matrix, which facilitates the deposition of Cu-Ni coated diamond particles. The tribological study indicates that both DMMC coatings exhibited super wear resistance performance. The super hard reinforcing diamond even resulted in severe wear and material loss of WC-Co pin ball. By comparing the two cold sprayed DMMC coatings, the DMMC-1 coating had better wear resistance properties than the DMMC-2 coating due to the higher diamond content and involvement of Cu and Ni.

Acknowledgments

The authors would like to thank the financial support from Irish Research Council project (GOIPD-2017-912). The authors also thank the CRANN Advanced Microscopy Laboratory (AML) of Trinity College Dublin for the support in the analysis.

References

1. S. Yin, C. Chen, X. Yan, X. Feng, R. Jenkins, and P.O. Reilly, The Influence of Aging Temperature and Aging Time on the Mechanical and Tribological Properties of Selective Laser Melted Maraging 18Ni-300 Steel, Addit. Manuf., Elsevier, 2018, 22(May), p 592–600, doi:10.1016/j.addma.2018.06.005.
2. A.P. Alkhimov, V.F. Kosareve, and A.N. Papyrin, A Method of Cold Gas-Dynamic Spray Deposition, Dokl. Akad. Nauk SSSR, 1990, 315(5), p 1062–1065.
3. S. Yin, X. Suo, Y. Xie, W. Li, R. Lupoi, and H. Liao, Effect of Substrate Temperature on Interfacial Bonding for Cold Spray of Ni onto Cu, J. Mater. Sci., Springer US, 2015, 50(22), p 7448–7457, doi:10.1007/s10853-015-9304-6.
4. S. Yin, Y. Xie, J. Cizek, E. Ekoi, T. Hussain, D. Dowling, and R. Lupoi, Advanced Diamond-Reinforced Metal Matrix Composites via Cold Spray: Properties and Deposition Mechanism, Compos. Part B Eng., Elsevier Ltd, 2017, 113, p 44–54, doi:10.1016/j.compositesb.2017.01.009.
5. L.-S. Wang, H.-F. Zhou, K.-J. Zhang, Y.-Y. Wang, C.-X. Li, X.-T. Luo, G.-J. Yang, and C.-J. Li, Effect of the Powder Particle Structure and Substrate Hardness during Vacuum Cold Spraying of Al2O3, Ceram. Int., Elsevier, 2017, 43(5), p 4390–4398, doi:10.1016/j.ceramint.2016.12.085.
6. C. Lee and J. Kim, Microstructure of Kinetic Spray Coatings: A Review, J. Therm. Spray Technol., 2015, 24(4), p 592–610, doi:10.1007/s11666-015-0223-5.
7. X.-T. Luo, C.-X. Li, F.-L. Shang, G.-J. Yang, Y.-Y. Wang, and C.-J. Li, High Velocity Impact Induced Microstructure Evolution during Deposition of Cold Spray Coatings: A Review, Surf. Coatings Technol., Elsevier B.V., 2014, 254, p 11–20, doi:10.1016/j.surfcoat.2014.06.006.
8. M.R. Rokni, S.R. Nutt, C.A. Widener, V.K. Champagne, and R.H. Hrabe, Review of Relationship Between Particle Deformation, Coating Microstructure, and Properties in High-Pressure Cold Spray, J. Therm. Spray Technol., Springer US, 2017, p 1–48, doi:10.1007/s11666-017-0575-0.
9. T. Klassen, H. Assadi, H. Kreye, and F. G, Cold Spraying e A Materials Perspective, Acta Mater., Elsevier Ltd, 2016, 116, p 382–407, doi:10.1016/j.actamat.2016.06.034.
10. A. M. Vilardell, N. Cinca, A. Concustell, S. Dosta, I.G. Cano, and J.M. Guilemany, Cold Spray as an Emerging Technology for Biocompatible and Antibacterial Coatings: State of Art, J. Mater. Sci., Springer US, 2015, p 4441–4462, doi:10.1007/s10853-015-9013-1.
11. .N. Raoelison, C. Verdy, and H. Liao, Cold Gas Dynamic Spray Additive Manufacturing Today: Deposit Possibilities, Technological Solutions and Viable Applications, Mater. Des., Elsevier Ltd, 2017, 133, p 266–287, doi:10.1016/j.matdes.2017.07.067.
12. W. Li, K. Yang, S. Yin, X. Yang, Y. Xu, and R. Lupoi, Solid-State Additive Manufacturing and Repairing by Cold Spraying: A Review, J. Mater. Sci. Technol., The editorial office of Journal of Materials Science & Technology, 2017, p 1–18, doi:https://doi.org/10.1016/j.jmst.2017.09.015.
13. K. Spencer, D.M. Fabijanic, and M.X. Zhang, The Use of Al-Al2O3 Cold Spray Coatings to Improve the Surface Properties of Magnesium Alloys, Surf. Coatings Technol., Elsevier B.V., 2009, 204(3), p 336–344, doi:10.1016/j.surfcoat.2009.07.032.
14. S. Kumar, S.K. Reddy, and S.V. Joshi, Microstructure and Performance of Cold Sprayed Al-SiC Composite Coatings with High Fraction of Particulates, Surf. Coatings Technol., Elsevier B.V., 2016, doi:10.1016/j.surfcoat.2016.11.047.
15. M. Yu, X.K. Suo, W.Y. Li, Y.Y. Wang, and H.L. Liao, Microstructure, Mechanical Property and Wear Performance of Cold Sprayed Al5056/SiCp Composite Coatings: Effect of Reinforcement Content, Appl. Surf. Sci., 2014, 289, p 188–196.
16. T. Peat, A. Galloway, A. Toumpis, P. McNutt, and N. Iqbal, The Erosion Performance of Particle Reinforced Metal Matrix Composite Coatings Produced by Co-Deposition Cold Gas Dynamic Spraying, Appl. Surf. Sci., Elsevier B.V., 2016, 396, p 1623–1634, doi:10.1016/j.apsusc.2016.10.155.
17. Y. Tao, T. Xiong, C. Sun, H. Jin, H. Du, and T. Li, Effect of α-Al2O3 on the Properties of Cold Sprayed Al/α-Al2O3 Composite Coatings on AZ91D Magnesium Alloy, Appl. Surf. Sci., 2009, 256(1), p 261–266.
18. A. Sova, A. Papyrin, and I. Smurov, Influence of Ceramic Powder Size on Process of Cermet Coating Formation by Cold Spray, J. Therm. Spray Technol., 2009, 18(4), p 633–641.
19. W.Y. Li, C. Yang, and H. Liao, Effect of Vacuum Heat Treatment on Microstructure and Microhardness of Cold-Sprayed TiN Particle-Reinforced Al Alloy-Based Composites, Mater. Des., Elsevier Ltd, 2011, 32(1), p 388–394, doi:10.1016/j.matdes.2010.06.002.
20. W.Y. Li, G. Zhang, H.L. Liao, and C. Coddet, Characterizations of Cold Sprayed TiN Particle Reinforced Al2319 Composite Coating, J. Mater. Process. Technol., 2008, 202(1–3), p 508–513.
21. P. Cavaliere, A. Perrone, and A. Silvello, Mechanical and Microstructural Behavior of Nanocomposites Produced via Cold Spray, Compos. Part B Eng., Elsevier Ltd, 2014, 67, p 326–331, doi:10.1016/j.compositesb.2014.07.023.
22. X.T. Luo and C.J. Li, Large Sized Cubic BN Reinforced Nanocomposite with Improved Abrasive Wear Resistance Deposited by Cold Spray, Mater. Des., Elsevier Ltd, 2015, 83, p 249–256, doi:10.1016/j.matdes.2015.06.009.
23. Meydanoglu, B. Jodoin, and E.S. Kayali, Microstructure, Mechanical Properties and Corrosion Performance of 7075 Al Matrix Ceramic Particle Reinforced Composite Coatings Produced by the Cold Gas Dynamic Spraying Process, Surf. Coatings Technol., Elsevier B.V., 2013, 235, p 108–116, doi:10.1016/j.surfcoat.2013.07.020.
24. P. Das, S. Paul, and P.P. Bandyopadhyay, Preparation of Diamond Reinforced Metal Powders as Thermal Spray Feedstock Using Ball Milling,

Surf. Coatings Technol., Elsevier B.V., 2016, 289, p 165–171, doi:10.1016/j.surfcoat.2015.12.022.
25. D.J. Woo, F.C. Heer, L.N. Brewer, J.P. Hooper, and S. Osswald, Synthesis of Nanodiamond-Reinforced Aluminum Metal Matrix Composites Using Cold-Spray Deposition, Carbon N. Y., Elsevier Ltd, 2015, 86, p 15–25, doi:10.1016/j.carbon.2015.01.010.
26. B. Aldwell, S. Yin, K.A. Mcdonnell, D. Trimble, T. Hussain, and R. Lupoi, A Novel Method for Metal – Diamond Composite Coating Deposition with Cold Spray and Formation Mechanism, Scr. Mater., Elsevier Ltd, 2016, 115, p 10–13, doi:10.1016/j.scriptamat.2015.12.028.
27. S. Dosta, M. Couto, and J.M. Guilemany, Cold Spray Deposition of a WC-25Co Cermet onto Al7075-T6 and Carbon Steel Substrates, Acta Mater., 2013, 61(2), p 643–652, doi:10.1016/j.actamat.2012.10.011.
28. L.Y. Chen, H. Konishi, A. Fehrenbacher, C. Ma, J.Q. Xu, H. Choi, H.F. Xu, F.E. Pfefferkorn, and X.C. Li, Novel Nanoprocessing Route for Bulk Graphene Nanoplatelets Reinforced Metal Matrix Nanocomposites, Scr. Mater., Acta Materialia Inc., 2012, 67(1), p 29–32, doi:10.1016/j.scriptamat.2012.03.013.
29. N. Yang, J. Boselli, and I. Sinclair, Simulation and Quantitative Assessment of Homogeneous and Inhomogeneous Particle Distributions in Particulate Metal Matrix Composites, J. Microsc., 2001, 201(2), p 189–200.
30. G. Iacob, V.G. Ghica, M. Buzatu, T. Buzatu, and M.I. Petrescu, Studies on Wear Rate and Micro-Hardness of the Al/Al2O3/Gr Hybrid Composites Produced via Powder Metallurgy, Compos. Part B Eng., 2014, 69, p 603–611.
31. W. Li, H. Assadi, F. Gaertner, S. Yin, W. Li, H. Assadi, F. Gaertner, and S. Yin, A Review of Advanced Composite and Nanostructured Coatings by Solid-State Cold Spraying Process A Review of Advanced Composite and Nanostructured Coatings by Solid-State Cold Spraying Process, Crit. Rev. SOLID STATE Mater. Sci., Taylor & Francis, 2018.
32. P.C. King, G. Bae, S.H. Zahiri, M. Jahedi, and C. Lee, An Experimental and Finite Element Study of Cold Spray Copper Impact onto Two Aluminum Substrates, J. Therm. Spray Technol., 2010, 19(3), p 620–634.
33. S. Guetta, M.H. Berger, F. Borit, V. Guipont, M. Jeandin, M. Boustie, Y. Ichikawa, K. Sakaguchi, and K. Ogawa, Influence of Particle Velocity on Adhesion of Cold-Sprayed Splats, J. Therm. Spray Technol., 2009, 18(3), p 331–342.
34. J.M. Shockley, S. Descartes, P. Vo, E. Irissou, and R.R. Chromik, The Influence of Al2O3 Particle Morphology on the Coating Formation and Dry Sliding Wear Behavior of Cold Sprayed Al–Al2O3 Composites, Surf. Coatings Technol., 2015, 270, p 324–333, doi:10.1016/j.surfcoat.2015.01.057.